desenvolvimento em QUESTÃO

EVALUATION OF FORMING LIMIT DIAGRAMS OF STAINLESS STEEL AISI 304 AND AISI 430

http://dx.doi.org/10.21527/2237-6453.2023.59.14301

Submitted: 11/4/2023
Accepted: 31/7/2023
Published: 30/11/2023

Rafael Pandolfo da Rocha,[1] Matheus Henrique Riffel,[2] Lirio Schaeffer[3]

ABSTRACT

Current quality standards require standardized tests in order to employ metal sheets in deep drawing processes. These tests are conducted aiming to assess their degree of formability in order to ensure that these materials can be formed without any defects such as wrinkling, earing, or even localized rupture. To evaluate whether a piece can be stamped without failures, the forming limit curve (FLC) is used, which provides data on the deformations that materials can withstand under certain modes of plastic deformation during stamping processes. In summary, the behavior of the maximum and minimum principal deformations of a stamped component is compared with the material's FLC: any combination located below the curve means deformations that the material can withstand, and consequently, those located above indicate its rupture. The objective of this article is to determine through experiments the FLCs of austenitic AISI 304 and ferritic AISI 430 stainless steels, using three different lubricants (Draw 58 GS, Neutron Super Corte 1123-21S, and Flash Stamp 140), in order to account for the influence of lubricants and, consequently, friction on the behavior of the forming limit curves. It was observed that the FLDs of AISI 304 and AISI 430 stainless steels are strongly sensitive to the employed lubricant types and, therefore, it directly influences the friction between tool and specimen. As the lubricant offered a reduction in the friction coefficient between the tribological pair during the modified Nakazima tests, there was an increase in the stampability of the AISI 304 stainless steel samples. On this behalf, the diagram was offset upwards. The lubricant Draw 58 GS offered the lowest friction coefficient among all the Other tested lubricants, guaranteeing an increase in the degree of stampability by approximately 20% and 30% in relation to the Neutron Super Corte 1123-21S and Flash Stamp 140 lubricants, respectively. In addition, small deviations were verified between the experimental curves and the curves provided by the literature for stainless steels AISI 304 and AISI 430. This could be explained by the difference in viscosity of the lubricants used in this study, affecting the behaviour of the FLDs. Finally, for both – experimental results and data provided by the literature – the parameters of the modified Nakazima test met the specifications from the ISO 12004:2008 standard.

Keywords: stainless steels; formability limit curve; modified Nakazima test; principal strains; deep drawing.

[1] Universidade Federal do Rio Grande do Sul. Programa de Pós-Graduação *Stricto Sensu* em Engenharia de Minas, Metalúrgica e Materiais. Porto Alegre/RS, Brasil. https://orcid.org/0009-0004-7835-5159

[2] Universidade Federal do Rio Grande do Sul. Porto Alegre/RS, Brasil. https://orcid.org/0009-0009-4639-0431

[3] Universidade Federal do Rio Grande do Sul. Programa de Pós-Graduação *Stricto Sensu* em Engenharia de Minas, Metalúrgica e Materiais. Porto Alegre/RS, Brasil. https://orcid.org/0000-0002-3427-2405

INTRODUCTION

The conformability of metallic materials reflects their ability to undergo plastic deformation until a certain form is achieved without defects. The most common defects that can occur during sheet metal forming processes are localized excessive thinning, fracture, wrinkling, or even significant degradation of surface quality. The existence of any of these defects can be considered as a limiting factor for formability and subsequently for the commercialization of stamped products. Currently, the Forming Limit Curve (FLC) is considered a widely used tool for the quantitative description of the formability of sheet metal (Banabic *et al*., 2013).

Keeler (1966) and Goodwin (1968) proposed a methodology to determine a forming limit curve expressed by pairs of principal strains associated with different modes of plastic deformation, developed under biaxial stress states of the "tension-tension," "tension-compression," and "compression-compression" type. Subsequently, research focused on improving the techniques used to print a grid of circles on the surface of the test specimens, measuring the principal strains and defining the limit strains, as well as developing suitable equipment and methodologies to explore the entire range of deformations of the samples (Banabic *et al*., 2013; Nakazima; Kikuma; Hasuka, 1968).

The FLC must cover the entire deformation domain specific to sheet metal stamping processes. In general, strain combinations vary between induced by uniaxial and induced by biaxial surface loads. The procedures used for the experimental determination of FLCs are carried out based on the stretching of the samples offered by puncture. Keeler (1966) was the first researcher to adopt this method, by using circular specimens and spherical punches with different radii aiming to modify the trajectory of deformations. In general, the puncture-strength test developed by Keeler investigates only the right side of FLC, characterized by uniaxial and/or biaxial stresses of the tensile type. Goodwin (1968) carried out different experiments simulating the deformation conditions occurring in mounting processes (simultaneous tensile and compressive stresses). In this way, he obtained critical deformation data referring to the left side of the curve (Allwod; Shouler, 2009).

Studies conducted by Nakazima, Kikuma and Hasuka (1968) improved these experimental procedures. He used a hemispherical punch with a constant radius, combined with rectangular specimens of different widths. In this way, Nakazima, Kikuma and Hasuka was able to explore both the stress domains of "compression-compression", "tension-compression" and "tension--tension" of the FLC. By using rectangular specimens with side notches, Hasek (1978) removed the main drawback of the Nakazima, Kikuma and Hasuka test, which was the wrinkling of the specimens due to stress concentration in the press sheet region. In this way, Hasek's study (1978) concentrated the deformations and, consequently, the ruptures in its central region (Banabic *et al.,* 2013).

FORMING LIMIT CURVE

The Forming Limit Curve (FLC) is considered a failure criterion because it indicates the limits between permissible and catastrophic deformations to which a sheet metal will be subjected during stamping procedures. Through the FLC curve, it is possible to predict the

deformations that will rupture the material considering the plastic deformation modes used in mounting processes (Silveira Netto, 2018).

The FLC describes the maximum limit of deformation that can occur in a sheet metal without its tightening or rupture, through the combination of its maximum () and minimum principal deformations (), in this way forming a diagram polynomial. The FLC curve presents the greatest deformations at the beginning of material failure (on the ordinate axis), as a function of the smallest deformations (on the abscissa axis), which are deformations that arise from tensile or compressive stresses. It is important to highlight that any combination of deformations below this curve represent safe stamping conditions, while the deformations above it can tighten or rupture the material. Figure 1 shows the plastic deformation modes in the FLC curve (represented by the deformation of the circles): stretching, plane deformation, uniaxial traction, deep embedding and uniaxial compression (Uthaisangsuk *et al*., 2008; Bhaduri, 2018).

Figure 1 – Forming Limit Curve and its respective deformation modes

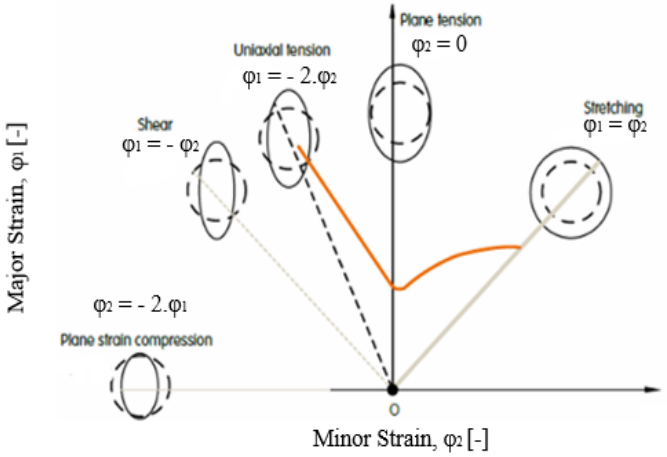

Fonte: Najmeddin; Javadimanesh (2013).

The test proposed by Nakazima, Kikuma and Hasuka (1968) is the most adopted to investigate and determine the deformation limit of sheet metal. This test includes the analysis of the stretching and embedding deformations and, therefore, describes the critical deformations for both sides of the FLC curve. The test consists of stretching samples of different widths until they break, using a hemispherical punch with a diameter of 100 mm. These samples remain between the matrix and the blank holder due to the application of a high load a wrinkle breaker (Figure 2). For the construction of the FLC, the pairs of maximum and minimum deformation close to the neck region are measured in each sample. These measurements are based on the deformation of small circles or squares that are printed on the surface of the material before the test is carried out (Li*, et al*., 2014; Ma *et al*., 2016).

Figure 2 – Nakazima test representation

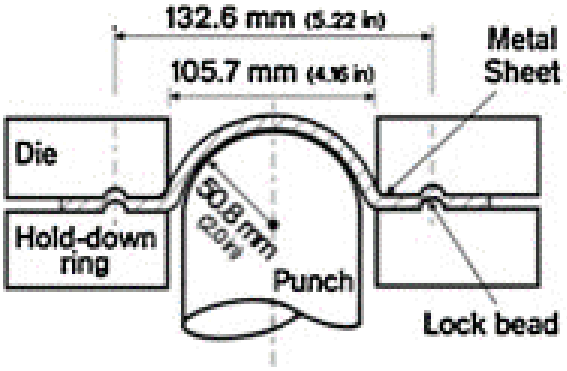

Fonte: Slota; Spisak (2015).

Although the test initially proposed by Nakazima, Kikuma and Hasuka (1968) used rectangular metal strips, other studies considered improvements to the test by applying the possibility of notching in these samples (Figure 3). These changes, in addition to forcing the tightening in the central region of the specimen, also increase the deformation widthwise. The deformation mode of the test specimen changes with the variation of its useful width, where smaller b_u samples develop deep drawing deformations, while larger b_u measurements correspond to biaxial stretching deformations. As the useful width increases, the deformation undergoes deep drawing, uniaxial tension, plane strain, stretching, and even biaxial stretching (Folle *et al.*, 2008).

Figure 3 – Shape and dimensions of the samples for the modified Nakazima test

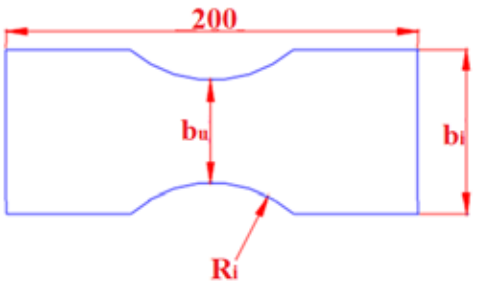

CP	R_i [mm]	b_u [mm]	b_i [mm]
1	100	10	40
2	90	20	50
3	80	30	60
4	70	40	70
5	60	50	80
6	50	60	100
7	40	80	120
8	25	100	150

Fonte: Silveira Netto (2018).

Below, the present study lists the main factors that can influence the behavior of the FLC curve, shifting it upwards or downwards. This means that they are responsible for increasing or reducing the stampability degree of the material (Silveira Netto, 2018; Folle *et al.*, 2008):

- Thickness: the higher the thickness of the sheet, the greater its ability to withstand plastic deformation. Consequently, there is an upward shift of the FLC curve.
- Friction: by reducing the friction coefficient, higher plastic deformations will be supported by the material without causing its rupture. Therefore, the FLC curve will be located higher.

- Rolling direction: specimens cut accordingly to the rolling direction have a greater capacity to withstand deformations, and when cut perpendicular to the rolling direction, they support less deformations.
- Anisotropy: within the conditions of $r_{90°} > r_{0°} > r_{45°}$ the material shows an increased deformation capacity in the 2nd quadrant and reduced in the 1st quadrant, causing the FLC curve to rotate clockwise.
- Pre-deformation: samples that have undergone tensile pre-deformations tend to generate a FLC curve positioned lower, whereas when the same samples are subjected to compressive pre-deformations, there is the generation of a higher FLC curve.
- Grain size: the smaller the grain size, the greater the formability of the material.
- Strain hardening index: the FLC curve tends to position itself higher for materials with higher strain hardening exponents.
- Punch velocity: the lower the velocity, the bigger are the plastic deformations that can be supported by the material.

Stress and strain behavior during deep drawing

Different modes of deformation act simultaneously during the stamping process of a cup, thus causing different states of stress and strain that occur radially, circumferentially, and normally (Figure 4). Usually, stress states can be analyzed in three different regions: in the flange, in the side wall, and in the bottom of the piece. The blank holder region is radially deformed into the die, accompanied by a reduction in its circumference and the application of compressive stresses in the circumferential direction and tensile stresses in the radial direction. The sides of the material are subjected to tensile stresses in the radial direction and zero stresses in the circumferential direction (plane strain state), causing its stretching and, as a consequence, the reduction of its thickness. In turn, the region located below the punch head shows thickness reduction as the sheet metal moves into the die, given the development of a biaxial state of tensile stresses (Folle, 2012).

Figure 4 – Representation of different stress states during deep drawing

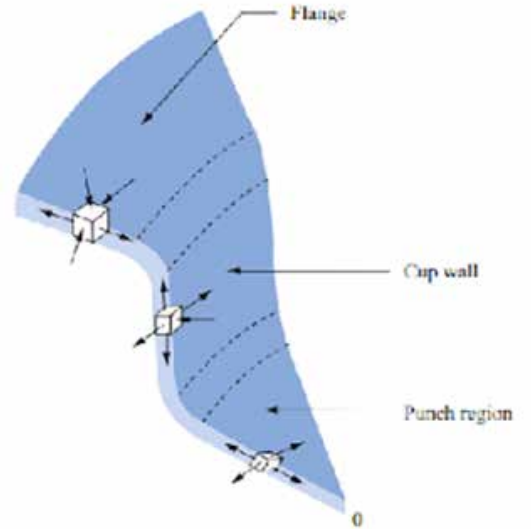

Fonte: Bhaduri (2018).

As the punch advances and contacts the central region of the blank, the material begins to settle over the punch head (bottom region of the cup), developing a biaxial state of tensile stress, a characteristic of the biaxial stretching deformation mode. The effect of normal stresses in this zone is not taken into account, once the contact established between the punch and the bottom of the piece is concentrated only in the region of the punch head radius. As a result, a small reduction in the thickness of the metal sheet is presented. In order to promote the flow of material into the cavity of the die, the friction must be high in the region of the punch head radius. On the other hand, it must be lower in other areas of contact between the metal and the tool to avoid problems such as defects in the final piece, equipment overload, and premature wear of the tools (Colgan; Monaghan, 2003; Dwivedi; Agnihotri, 2017).

The material located at the end of the cup (flange region), once subjected to the deformation mode by drawing, moves inward into the die cavity because of tensile stresses in the radial direction. Due to the progressive reduction of the circumference of the flange, compressive stresses arise in the circumferential direction. When these stresses reach a certain limit, they give rise to wrinkles that, if transferred to the die cavity, can lead to stress concentration in the vicinity of the punch head radius and, consequently, to early failure of the part. To avoid this type of defect, the press develops compressive stresses in the normal direction, which, combined with tensile and compressive stresses in the radial and circumferential directions, respectively, cause an increase in the thickness of the flange (Folle, 2012).

As the material slides into the die, the metal is bent and subsequently unbent in the entry radius region. This effect happens due to the stretching caused by tensile stresses located on the inner wall of the cup. The load applied to the bottom of the cup is transferred to its inner wall, resulting in a state of plane deformation and, consequently, tensile stresses that not only homogenize the thickness but also accentuate its reduction. If the clearance between the punch and the die is less than 10% or 20% of the generator thickness, the thickness reduction phenomenon will be even more severe, resulting in rupture in the vicinity of the cup top. In addition to increasing the clearance between the die and the punch, this defect can be corrected by increasing the radius of the punch head and reducing the applied load during the stamping process (Olsson; Bay; Andreasen, 2010; Zaid, 2017).

Main deformation modes in stamping processes

The FLC identifies the possible modes of plastic deformation during sheet metal forming processes: biaxial stretching, planar deformation, uniaxial tensile, pure deep drawing or shearing, and uniaxial compression (Karima; Chandrasekaran; Tse, 1989; Hu; Marciniak; Duncan, 2002; Rocha, 2006). The biaxial stretching deformation mode is characterized by the fact that the maximum (σ_1) and minimum (σ_2) principal stresses are equal, and both developing under a tensile nature, causing the circles printed on the surface of the sheet to deform by expansion. This typically occurs in the portion of the sheet that deforms in the border region near the punch head (Figure 5), and it is associated with thinning of the metal sheet. The magnitude of the deformation is sensitive to the resistive force of the sheet sliding into the die (due to the action of the blank holder), as well as the punch head radius and the die entry radius (Karima; Chandrasekaran; Tse, 1989; Hu; Marciniak; Duncan, 2002; Rocha, 2006).

Figure 5 – Biaxial stretching deformation mode.

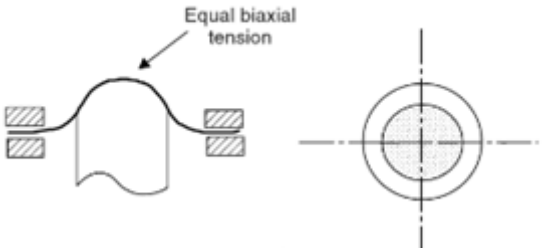

Fonte: Hu; Marciniak; Duncan (2002).

The stage of plane strain deformation usually occurs on the walls of the material during stamping (Figure 6), and it is characterized by the development of tensile stresses in the radial direction and zero in the circumferential direction. The stamped circles on the material's surface become ellipses after the forming process, remaining their width (circumferential direction) unchanged. These tensile stresses happen due to the restriction of material slippage into the mold, caused by the action of friction and/or the press force. In the FLC curve, it is possible to highlight that, among all, the plane strain deformation mode gives the material the lowest formability limit.

Figure 6 – Plane strain deformation mode

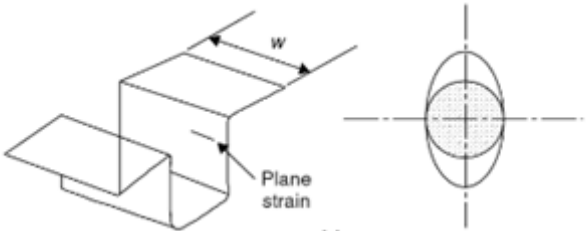

Fonte: Hu; Marciniak; Duncan (2002).

The deformation by uniaxial tension mode corresponds to the transition zone between the plane strain deformation mode and the deep drawing mode. This deformation mode is typically found in specimens subjected to tensile testing, and is occurs by the action of tensile stresses in the longitudinal direction, while no other stresses are perceptible in the other directions. ($\sigma_2 = \sigma_3 = 0$). Therefore, there is elongation of the material length, along with a reduction of its cross-sectional area. In addition, it can arise during the expansion of holes in metal sheets, whenever a free edge is stretched (Figure 7) (Karima; Chandrasekaran; Tse, 1989; Hu; Marciniak; Duncan, 2002; Rocha, 2006; Gilapa, 2011).

Figure 7 – Deformation by uniaxial tension mode

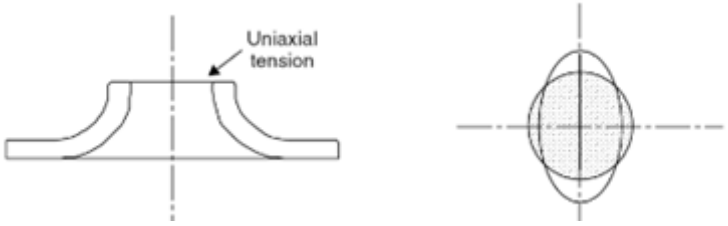

Fonte: Hu; Marciniak; Duncan (2002).

The Pure Shearing or Deep Drawing Mode is considered the ideal plastic deformation mode, and it is characterized by tensile stresses acting in the radial direction and compressive stresses in the circumferential direction (Figure 8). This mode commonly happens in the flange region (press-chip region), where the tensile stresses are compensated by the compressive stresses, ensuring that the thickness of the material remains constant during its sliding into the die. Given that there is no deformation along the thickness ($\varphi_3 = 0$) and the principal stresses are low (representing about 58% of the yield stress), there is no possibility of failure in this zone (Karima; Chandrasekaran; Tse, 1989; Hu; Marciniak; Duncan, 2002; Rocha, 2006; Gilapa, 2011).

Figure 8 – The Pure Shearing or Deep Drawing Mode

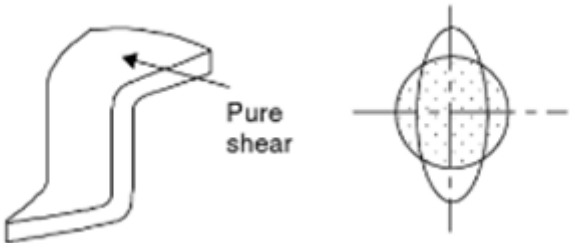

Fonte: Hu; Marciniak; Duncan (2002).

Deformation configuration by uniaxial compression occurs in the outer edge of the flange, with compressive stresses in the circumferential direction (σ_2) that overlap with tensile stresses in the radial direction (σ_1). As a result of this process, the material thickness tends to increase at the end of the flange, significantly reducing the contact of the press with the remaining area of the flange. Moreover, wrinkles may arise in this region of the flange, resulting from the intensity of these circumferential compressive stresses. It is assumed that for this severe deformation condition, the maximum principal stresses are nonexistent ($\sigma_1 = 0$), while the minimum principal stresses take on the value of the yield stress ($\sigma_2 = -\sigma_{eq} = -kf$) (Hu; Marciniak; Duncan, 2002; Rocha, 2006; Gilapa, 2011).

Figure 9 – Uniaxial compression deformation mode

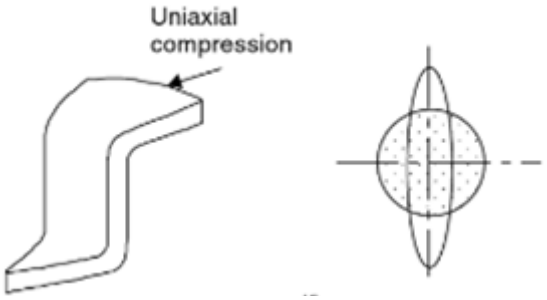

Fonte: Hu; Marciniak; Duncan (2002).

MATERIALS AND METHODS

The present study adopted the modified Nakazima test to construct the Limiting Drawing Ratio (LDR) curves for AISI 304 and AISI 430 stainless steels, using tools and samples with standardized geometries (Figures 2 and 3, respectively), according to ISO 12004 (2008a) standard. During the test, eight types of specimens with a thickness of 1 mm were tested, with

variations in their useful width (b_u), aiming to promote different modes of plastic deformation in the material and, consequently, determine their respective deformation limits.

The surfaces of the samples were engraved with a grid of circles with diameters of 2.5 mm, using electrochemical etching (a technique called viscoplasticity). The electrochemical etching is conducted using a 12V power source, a carbon engraving head, a piece of felt, a specific electrolyte for stainless steels, and a Nylon screen with the pattern of the circle grid to be printed. The engraving head is connected to the positive pole of the power source and it is also covered by the felt soaked with the electrolyte. The Nylon screen is placed over the sample, which is connected to the negative pole of the power source, thus closing the circuit. As soon as the engraving head contacts the Nylon screen and the metal plate, the electric current passes through the screen and the plate, promoting the electrochemical corrosion of the surface of the samples in the shape of circles, due to the joint action of the electrolyte (Figure 10).

Figure 10 – Illustration of the electrochemical etching process

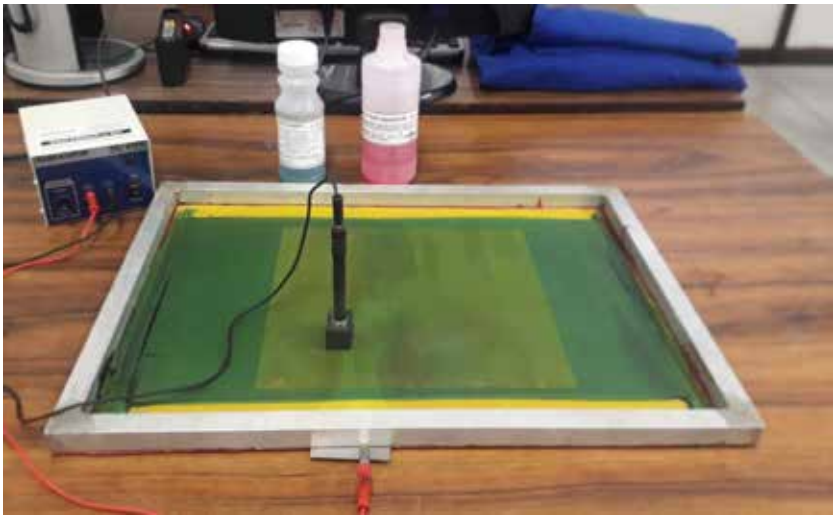

Fonte: Authors (2023).

After the etching of the circle mesh, the modified Nakazima test is performed on the EMIC machine at the Laboratory of Mechanical Transformation (LdTM) of the Federal University of Rio Grande do Sul (UFRGS). The present study fixed the samples between the die and the press plate by a force high enough to prevent material slippage into the die cavity (Figure 11). The punch moves towards the sample at a constant speed of 1.5 mm/s, causing its elongation, according to ISO 12004:2008 standard. Three types of lubricants (Draw 58 GS, Neutron Super Cut 1123-21S and Flash Stamp 140) were used for lubrication of the contact established between the material surfaces and the tools. In summary, three tests were performed for each sample type, for each material, and for each lubricant used, reaching a total of 144 tests.

Figure 11 – Representation of the modified Nakazima test performed on the EMIC machine

Fonte: Authors (2023).

The principal deformations are measured from the plastic deformation of the circles etched onto the surfaces of the specimens which, after the Nakazima test, become ellipses (Figure 12). By varying their initial diameter (d_0), it is possible to determine the maximum (φ_1) and minimum (φ_2) principal deformations at the points bordering the necking zone (Hu; Marciniak; Duncan, 2002).

Figure 12 – Measurement of principal deformations using the visioplasticity technique

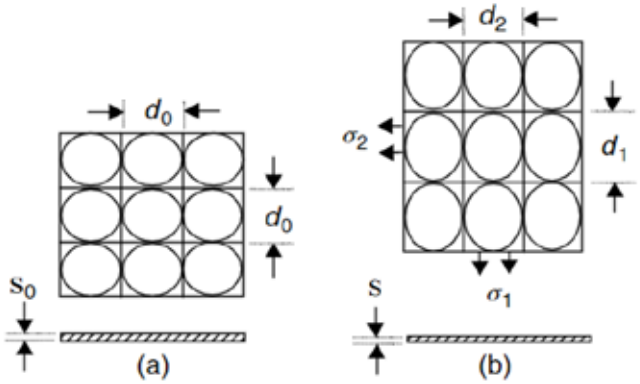

Fonte: Hu; Marciniak; Duncan (2002).

The principal deformations φ_1 and φ_2 are calculated using equations 1 and 2 (Folle *et al.*, 2008).

$$\varphi_1 = ln\ ln\left(\frac{d_1}{d_0}\right) \quad (1)$$

$$\varphi_2 = ln\ ln\left(\frac{d_2}{d_0}\right) \quad (2)$$

The tests ended as soon as a localized necking was observed on the samples (Figure 13). Two ellipses must be measured for each sample type, one on each side of the necking. The measured ellipse should be the one closest to the necking, provided it is complete, that is, it has maintained the integrity of its contour line (Folle *et al*., 2008).

Figure 13 – Representation of the samples after the modified Nakazima test

Fonte: Authors (2023).

In order to measure the deformation of the ellipses, a flexible and transparent ruler was used, graduated with relative (ε) and true (φ) deformations for the 2.5 mm diameter grid (Figure 14). The ruler permits direct reading of these deformations in addition to being flexible and transparent, it follows the shape of the specimens after the Nakazima test and allows for measurement of the deformation of the circles. The readings of the principal deformations occur when the transverse lines of the ruler have the same dimension as the length and width of the ellipse, which correspond to the maximum (φ_1) and minimum (φ_2), principal deformations, respectively (Folle *et al*., 2008).

Figure 14 – Flexible and transparent ruler used to measure deformations

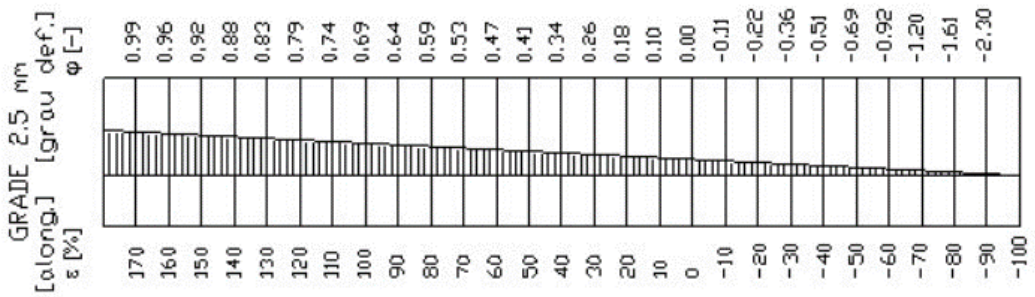

Fonte: Silveira Netto (2018).

RESULTS

Figures 15 and 16 show the FLC curves of AISI 304 and AISI 430 stainless steels for each lubricant used during the modified Nakazima test, which correspond to the trend lines of the maximum (φ_1) and minimum (φ_2) principal deformations measured and later plotted in MS Excel software.

Figure 15 – FLC curves of AISI 304 stainless steel for each type of lubricant

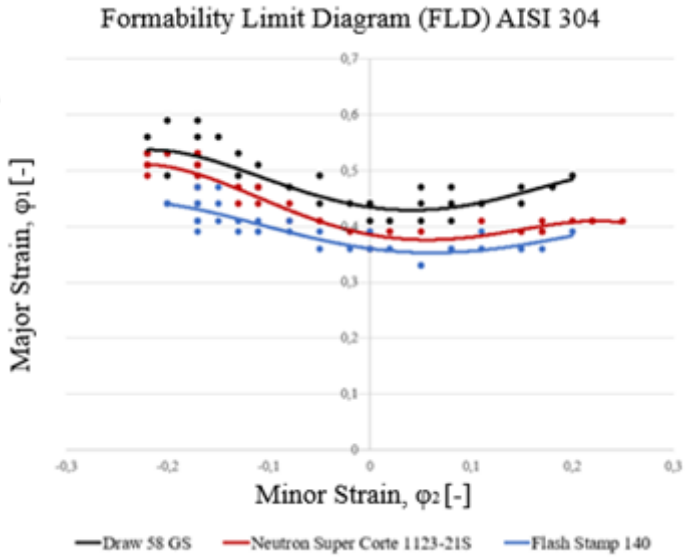

Fonte: Authors (2023).

Figure 16 – FLC curves of AISI 430 stainless steel for each type of lubricant

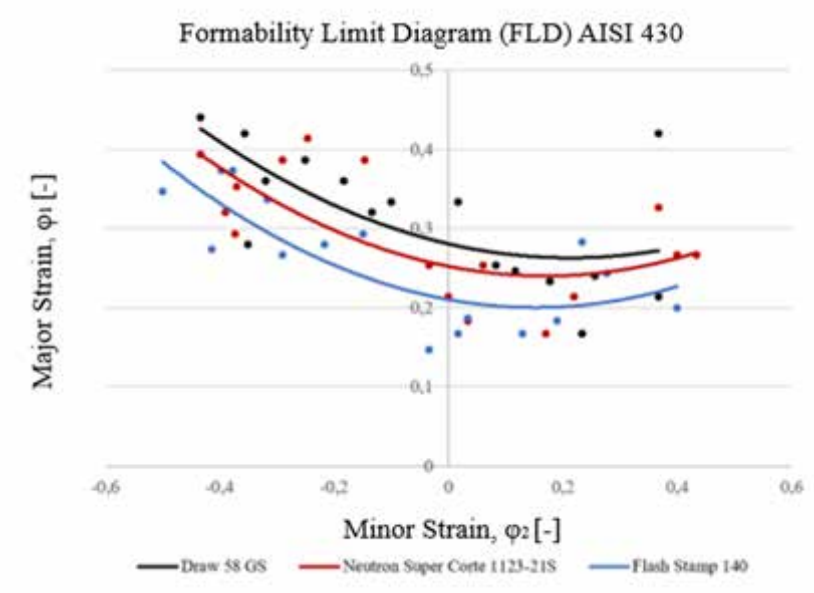

Fonte: Authors (2023).

It was ascertained that the use of Draw 58 GS lubricant offered the lowest coefficient of friction compared to the other lubricants used, ensuring an increase in the degree of formability by approximately 20% and 30% compared to the lubricants Neutron Super Cut 1123-21S and Flash Stamp 140, respectively.

Moreover, the experimentally found FLCs for the AISI 304 stainless steel are similar to the results obtained in the works of Schino (2019) (Figure 17), Cardoso *et al.* (2013) (Figure 18), and Cavaler (2010) (Figure 19).

Figure 17 – FLCs of AISI 304 stainless steel for each type of lubricant

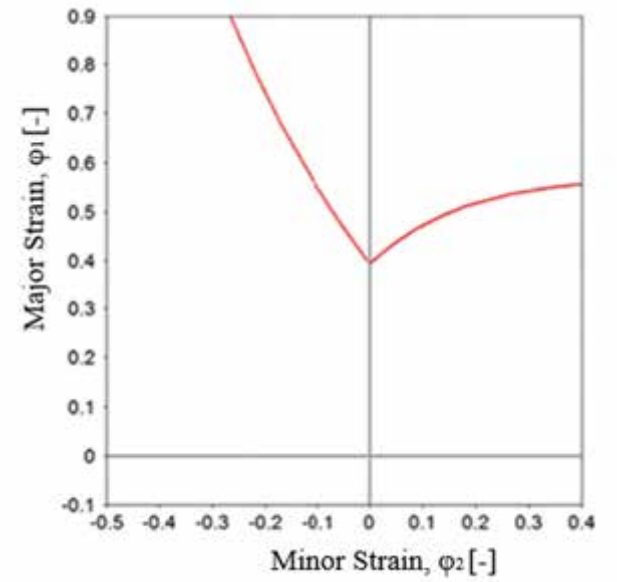

Fonte: Schino (2012).

Figure 18 – Forming Limit Curve of AISI 304 Stainless Steel

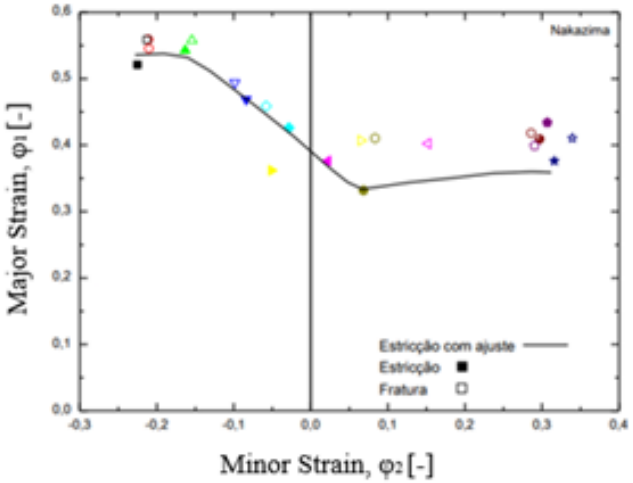

Fonte: Cardoso *et al*. (2013).

Figure 19 – Forming Limit Curve of AISI 304 Stainless Steel

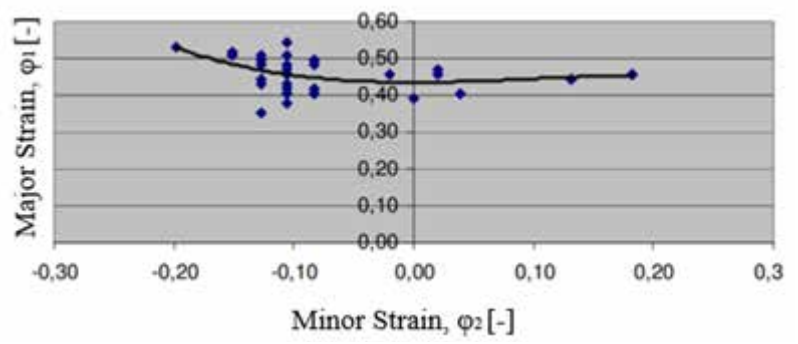

Fonte: Cavaler (2010).

On the other hand, the FLCs for AISI 430 stainless steel found through experiments appear to be similar to the results obtained in the works of Carneiro *et al.* (2016) (Figure 20), Luiz; Rodrigues (2022) (Figure 21), and Bong *et al.* (2012) (Figure 22).

Figure 20 – Forming Limit Curve of AISI 430 Stainless Steel

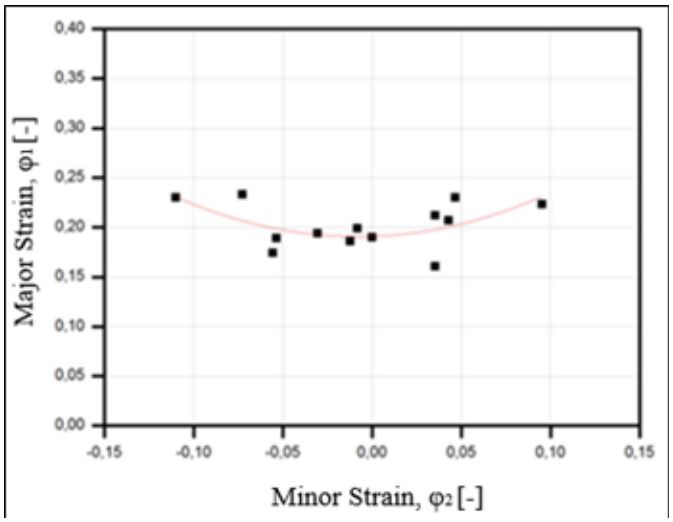

Fonte: Carneiro *et al.* (2016).

Figure 21 – Forming Limit Curve of AISI 430 Stainless Steel

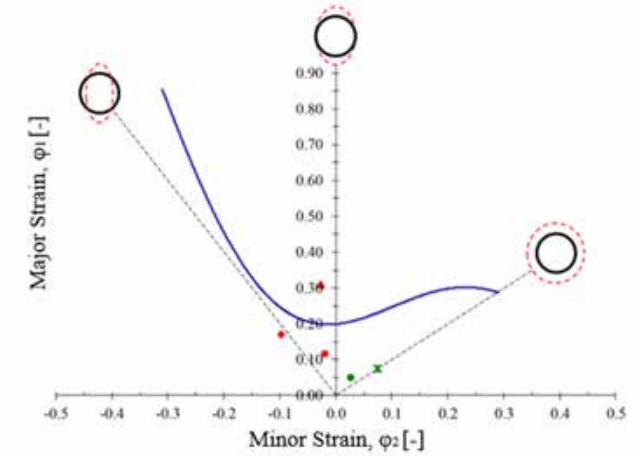

Fonte: Luiz; Rodrigues (2022).

Figure 22 – Forming Limit Curve of AISI 430 Stainless Steel

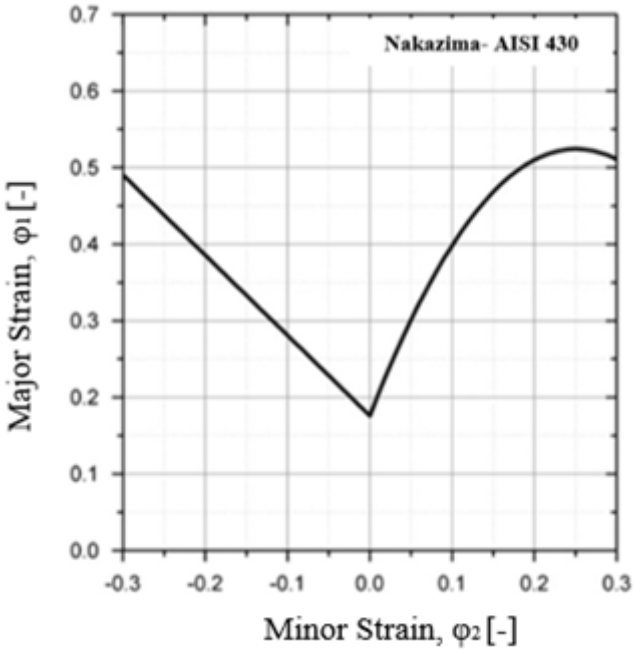

Fonte: Bong *et al* (2012).

The difference between the experimental curves and the curves provided by the literature for AISI 304 and AISI 430 stainless steels is justified by the viscosity of the lubricants used and, consequently, the friction in each test. Besides, both for the experiments in the present study and in the literature, the parameters of the modified Nakazima test complied with the specifications of the ISO 12004 (2008b) standard. In addition, possible discrepancies between the mechanical properties of the samples in this study and those in the literature, such as the strain hardening exponent and the yield and ultimate tensile strength limits, can contribute to significant differences in the shape of the FLCs.

FINAL REMARKS

Therefore, this study's contribution to the academic and industrial sectors is highlighted with regard to the validation of the modified Nakajima Test to determine the stampability limits of AISI 304 and 430 stainless steels. Further, this study presents the main modes of plastic deformation that can be developed on a sheet metal during deep drawing processing. The FLDs´ results provided by this work can be implemented in numerical simulation softwares in order predict the plastic behaviour of such stainless steels during the stamping processes. This is particularly useful, for the industrial and academic communities, to improve the main parameters of the stamping process or for optimize the tooling design. At the same time, the "trial & error" technique, which is still widely widespread by the industry during the tooling design and/or the deep drawing process process itself, will be gradually discarded. Such evolution will aid to avoid the waste of raw material caused by processing defects, such as wrinkling, earing and localized rupture.

Forming limit curves predict the limit of deformation that materials can withstand before reaching their breaking point. Typically, this data serves as a parameter for the design of

stamped products, considering that for any region, the principal strain pairs must lie below the FLC, ensuring the structural integrity of the parts for their final application. It is worth noting that numerous commercial software programs can already predict the configuration of metal sheet FLCs, requiring only information related to the thickness, strain hardening index, yield and ultimate strengths of the material. Nevertheless, the influence of lubricants and, consequently, friction on the final configuration of FLCs makes it difficult for these software programs to accurately describe the final results. This happens because most softwares consider friction as a constant variable during forming processes, neglecting the influence exerted by different factors, such as lubricant viscosity, tool sliding velocity and pressure in each region of the part during its permanent deformation.

Through Figures 15 and 16, the present study indicates that FLCs are highly susceptible to changes in the type of lubricant used and, consequently, to friction, as already supported by the studies of Silveira Netto (2018) and Folle *et al.* (2008). As the lubricant offered a reduction in the coefficient between the tools and the samples during the modified Nakazima tests, there was an increase in the formability of the AISI 304 and AISI 430 stainless steel sheets, thus shifting the limit curve upwards. In summary, the use of the Draw 58 GS lubricant offered the lowest friction coefficient compared to the other lubricants used, ensuring an increase in formability of approximately 20% and 30% compared to the Neutron Super Corte 1123-21S and Flash Stamp 140 lubricants, respectively. Additionally, the present study identified that the formability of AISI 304 stainless steel is superior to that of AISI 430, since the CLCs of AISI 304 were located much higher than the curves of AISI 430.

ACKNOWLEDGMENTS

The authors would like to thank the Federal University of Rio Grande do Sul (UFRGS) for the infrastructure provided for the experimental tests, as well as the National Council for Scientific and Technological Development (CNPq) and the Coordination for the Improvement of Higher Education Personnel (Capes) for the scholarships that support the development of national scientific research.

REFERENCES

ALLWOOD, J. M.; SHOULER, D. R. Generalised forming limit diagrams showing increased forming limits with non-planar stress states. *International Journal of Plasticity*, v. 25, p. 1.207-1.230, 2009.

BANABIC, D. *et al*. Development of a new procedure for the experimental determination of the Forming Limit Curves. *Cirp Annals: Manufacturing Technology,* Cluj-Napoca, p. 255-258, 2013.

BHADURI, A. *Mechanical properties and working of metals and alloys*. Singapore: Springer Singapore, 2018. p. 748.

BONG, H. J. *et al*. The forming limit diagram of ferritic stainless steel sheets: experiments and modeling. *International Journal Of Mechanical Sciences*, Gyeongbuk, v. 64, p. 1-10, 2012.

CARDOSO, M. C. *et al. Avaliação da curva limite de conformação de um aço inoxidável austenítico*. CONGRESSO BRASILEIRO DE ENGENHARIA DE FABRICAÇÃO, 7., 2013, Itatiaia, 2013. p. 1-10.

CARNEIRO, J. P. S. *et al*. *Comparative study of formability and mechanical properties of AISI 316 and AISI 430 stainless steel*. INTERNATIONAL CONFERENCE ON INTEGRITY-RELIABILITY-FAILURE, 5., 2016, Porto, 2016. p. 213-220.

CAVALER, L. C. C. *Parâmetros de conformação para a estampagem incremental de chapas de aço inoxidável AISI 304L*. 2010. 152 p. Tese (Doutorado Acadêmico) – Programa de Pós-Graduação em Engenharia de Minas, Metalúrgica e de Materiais – PPGE3M, Universidade Federal do Rio Grande do Sul, Porto Alegre, 2010.

COLGAN, M.; MONAGHAN, J. Deep drawing process: analysis and experimente. *Journal of Materials Processing Technology*, v. 132, p. 25-41, 2003.

DWIVEDI, R.; AGNIHOTRI, G. Study of deep drawing process parameters. INTERNATIONAL CONFERENCE OF MATERIALS PROCESSING AND CHARACTERIZATION (ICMPC, 2016), 5., 2017, Bhopal: Índia, 2017. p. 820-826.

FOLLE, L. F. *Estudo do coeficiente de atrito para processos de estampagem*. 131 p. Tese (Doutorado Acadêmico) – Programa de Pós-Graduação em Engenharia de Minas, Metalúrgica e de Materiais – PPGE3M, Universidade Federal do Rio Grande do Sul, Porto Alegre, 2012.

FOLLE, L. F. *et al*. Escolha do lubrificante correto torna mais precisa a curva-limite de conformação. *Corte e Conformação de Metais*, 37, p. 64-76, abr. 2008.

GILAPA, L. C. M. *Efeito do teor de cobre e dos caminhos de deformação na conformabilidade e na martensita induzida por deformação no aço inoxidável austenítico AISI 304.* p. 130. Tese (Doutorado Acadêmico) – Universidade Federal de Santa Catarina, Programa de Pós-Graduação em Ciência e Engenharia de Materiais, Joinvile, 2011.

GOODWIN, G. M. Application of strain analysis to sheet metal forming problems in the press shop. *SAE Transactions*, p. 380-387, 1968.

HASEK, V. Untersuchung und theoretische Beschreibung wichtiger Einflussgrossen auf das Grenzformaenderungschaubild. *Blech 25,* v. 5, v. 6, v. 10, v. 12), p. 213-220, p. 285-292, p. 493-499, p. 619-627, 1978.

HU, S. J.; MARCINIAK, Z.; DUNCAN, J. L. *Mechanics of sheet metal forming*. Woburn: Elsevier Science, 2002.

ISO. International Organization for Standardization. *ISO 12004-1*: Measurement and application of forminglimit diagrams in the press shop. Geneva, 2008a. 16 p.

ISO. International Organization for Standardization. *ISO 12004-2:* Determination of forming-limit curves in the laboratory. Geneva, 34 p., 2008b.

KARIMA, M.; CHANDRASEKARAN, N.; TSE, W. Process signatures in metal stamping: Basic concepts. *J. Mater. Shaping Technol*, v. 7, p. 169-183, 1989.

KEELER, S. Determination of forming limits in automotive stampings. *SAE Transactions*, 74 p. 1-9, 1966.

LI, F.F. *et al*. Experimental and theoretical study on the hot forming limit of 22MnB5 steel. *The International Journal of Advanced Manufacturing Technology*, v. 71, p. 297-306, 2014.

LUIZ, V. D.; RODRIGUES, P. C. de M. Failure analysis of AISI 430 stainless steel sheet under stretching and bending conditions. *The International Journal of Advanced Manufacturing Technology*, London, v. 121, p. 2.759-2.772, 2022.

MA, B. *et al*. Prediction of forming limit in DP590 steel sheet forming: An extended fracture criterion. *Meterials and Design*, v. 96, p. 401-408, 2016.

NAKAZIMA, K.; KIKUMA, T.; HASUKA, K. Study on the formability of steel sheets. *Yamata Technical Report,* v. 264, p. 8.517-8.530, 1968.

NAJMEDDIN, A.; JAVADIMANESH, A. Theoretical and experimental analysis of deep drawing cylindrical cup. *Journal of Minerals and Materials Characterization and Engineering*, v. 1, p. 336-342, 2013.

OLSSON, D. D.; BAY, N.; ANDREASEN, J. L. A quantitative lubricant test for deep drawing. *International Journal of Surface Science And Engineering*, Mariager, p. 2-12, 2010.

ROCHA, M. R. *Estudos da conformabilidade dos aços inoxidáveis austeníticos 304N e 304H e suas correlações com as microestruturas obtidas*. p. 154. Tese (Doutorado Acadêmico) – Universidade Federal de Santa Catarina, Programa de Pós-Graduação em Ciência e Engenharia de Materiais, Joinvile, 2006.

SCHINO, A. di. Advances in materials science and engineering: prediction of AISI 304 stainless steel pipe deformation by FEM simulation. *Metallurgist*, Moscow, v. 63, p. 511-520, 2019.

SILVEIRA NETTO, S. E. *Desenvolvimento do processo de construção de curvas limite de conformação*. 2018. 90 p. Dissertação (Mestrado Acadêmico) – Universidade Federal do Rio Grande do Sul, Programa de Pós-Graduação em Engenharia de Minas, Metalúrgica e de Materiais – PPGE3M, Porto Alegre, 2018.

SLOTA, J.; SPISAK, E. Experimental FLC determination on high strength steel sheet metal. *Acta Metallurgica Slovaca,* v. 21, n. 4. p. 269-277, 2015.

UTHAISANGSUK, V. *et al.* Experimental and numerical failure criterion for formability prediction in sheet metal forming. *Computational Materials Science*, v. 43, p. 43-50, 2008.

ZAID, A. I. O. Effect of diferente lubricants on deep drawing of galvanized steel. International. *Journal of Scientific & Engineering Research*, v. 8, 2017.

Autor correspondente:
Rafael Pandolfo da Rocha
Universidade Federal do Rio Grande do Sul. Programa de Pós-Graduação Stricto Sensu em Engenharia de Minas, Metalúrgica e Materiais – PPGE3M
Av. Bento Gonçalves, 9500 - setor IV, Bairro Agronomia, Porto Alegre/RS, Brasil. CEP 90650-001
E-mail: rafael.pandolfo@ufrgs.br